



Effect of swirl gas injection on bubble characteristics in a bubble column

Ariny Demong^{1,*}, Andrew Ragai Rigit², Khairuddin Sanaullah¹

¹ Department of Chemical and Energy Sustainability, Faculty of Engineering, Universiti Malaysia Sarawak (UNIMAS), Malaysia

² Department of Mechanical and Manufacturing Engineering, Faculty of Engineering, Universiti Malaysia Sarawak (UNIMAS), Malaysia

ABSTRACT

The attempt of this study is to obtain an effect of swirl gas injection on bubble characteristics, such as bubble share, size and velocity. A bubble detection technique has been developed for fast and accurate measurement of bubble size distributions on gas – liquid two systems. This techniques use advance digital image processing consists of edge detection and bubble edge recognition. Measurements are also carried out in mixing vessels to study the effect of impeller speed and gas sparging rate on the bubble size and its distributions. The investigation are carried out in a bubble column characterized with 57 cm and 61 cm height. The column was made of Plexiglas and equipped with a ring sparger. The top of the column was opened to atmosphere. The liquids used was tap water and the gas phase was air from air compressor. A high speed digital camera is employed for the measurement of the rise velocity of bubbles and etc. Bubble size decreased with increase in impeller speed, whereas the bubble population is increase as the sparger rotating speed increase from 30 rpm to 150 rpm.

Keywords:

Bubble detection technique; image analysis; bubble size; population

1. Introduction

In few decades, the motion of bubble rising in liquids has been pay attention of researchers because of bubble fascinating variety of motion patterns and instabilities. In two-phase bubbly flows, bubbles have a shape of spheres, ellipsoids or spherical caps, which they rise in rectilinear, spiraling, zigzagging, or rocking motion depends on the characteristics of the system such as bubble diameter and the properties of the liquid [1,2]. At the point where gas is injected into a stagnant liquid, bubbles are formed and rapidly move upward due to buoyancy force. As the bubble size increases, the bubble shape changes from spherical to ellipsoidal and after that to a spherical cap. There are three component cause bubble to breakup, for example, instabilities of larger bubbles, detaching the edges of larger bubble and collisions between bubbles [3]. The bubble will either reduce or increase in size due to coalescence or break-up as it rises through the column. There are few factors that can affect the shape of the bubbles, such as, fluid density, fluid viscosity, surface tension, terminal gas velocity, gravitational acceleration, etc. This change in bubble size occurs when the bubble is subjected to these external factors until the forces balance at the gas-fluid interface.

Detailed quantitative studied of the flow evolution in the wake of bubbles and swarms are difficult due to the instabilities of the flow. Our current work attempts to describe the structure of

* Corresponding author.

E-mail address: arinydemong91@gmail.com

the wake of free rising bubbles and its effect on the bubble interaction in a more detailed way. In the experiments describe herein, a high speed camera was used to obtain the temporal evolution of the flow fields in bubbly flows. The dispersion of gas into a liquid relies upon the bubble size, and the distribution of the bubble possibly it coalesces or breakup [4]. Bubble size can be increased through coalescence, which two or more bubbles coming together. There are three mechanisms of bubble coalescence, such as, bubble coalesce because of turbulence; different bubbles size toward each other, and one of the bubble being drawn into the wake of a preceding one [3,5]. Buwa and Ranade (2002) presented experimental data similar to that of Mudde *et al.*(1997) on dynamics of gas-liquid flows using different sprayer's configurations and different liquids. Their results suggested that the bubbles size distribution is the key parameter that controls the dynamic characteristics of the bubble column [6,7]. Hibiki *et al.*(2001) and Sun *et al.*(2004) developed a double sensor probe based on the concept of interfacial area concentration, the gas velocity and bubble Sauter mean diameter in a 3-D bubble column [8,9].

The aim of this research is the characterization of bubble in bubbly flow under presence of swirl sparging, i.e presence of various rpm of sparger rotation in the range 30 to 150 rpm. To achieve these objectives required development of measurement techniques of bubble surface oscillations; characterization of bubble interactions, and evaluation of the effect of gas sparging rate and rotating speed. These required development of appropriate images processing technique.

2. Methodology

The investigation was carried out in a bubble column (diameter 57cm, and 61cm height). The experimental setup is illustrated in Figure 1 and it consists of a column made of Plexiglas, was equipped with ring sparger. The column also equipped with appropriate motor for the rotating of the sparger at the bottom of the column. All the experiments were conducted at ambient temperature and pressure conditions. The liquids used was tap water and the gas phase was air from air compressor. The ring sparger has 190 holes with diameter of 1mm, and thickness of 0.5mm. The experiments were performed at gas flow rate ranging from 0.063 g/s to 0.316 g/s. The gas flow rate was measure using gas flow meter. Each experiments run is initiated by string the gas supply and then filling the water up to 50 cm above the sparger.

Descriptions, development and validation of methods are presented for techniques created or adapted to characterize the bubble motion. These techniques are High speed cinematography, conversion of bubble images into data structure, tracking of multiple moving bubble, bubble trajectory reconstruction and bubble velocity measurements.

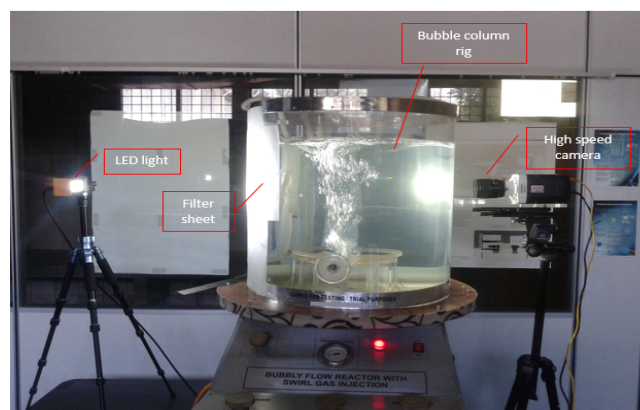


Fig. 1. Experimental setup for bubbly flow visualization

A high speed camera is placed in front of the bubble column rig a LED light at the other side of bubble column. Filter paper is stuck on the opposite wall of the bubble column (in front of LED light) to avoid undesired reflections and refractions as much as possible. Then, the bubble column with tap water until 50 cm height. Bubbles is let to pass through the sparger and rise in bubble column at some time in stagnant water. Then, the image of the bubble rise is captured at desired height started from the bottom of the bubble column. The focus lens of the camera is adjusted to get a clear image. The high speed camera is set at 800 frame rate per second with a full mode, which the resolution of 1024 x 768 pixels. The videography of the bubbly flow is captured and saved on the desktop in a file. Then, the images are processed using an image software or programming to get a data of bubble size and bubble velocity.

A high speed digital video camera (Phantom) is employed for the measurement of the rise velocity, bubble size and etc. The camera is fixed on a stand very close to the area of observation in such a way that the test area is located between the camera and an appropriate lighting system. By using an appropriate software (Matlab, Image J), the rise velocity, bubble size and shape can be obtained from the recorded images. The difference in gas flow rate and rotating speed of the sparger are taken as the reading. The images captured from the high speed camera are processed in three steps, such as image color formatting, bubble detection and measurement of bubble characteristics.

The image captured changes in color known as raw images. Then, from the raw image, the RGB (red, green and blue) format is extracted and from RGB image, construct the black and white image. Then, subtract the background image to process the shadow image for analysis. From the shadow image, the contour of the bubble is tracked accurately. The image captured is processed by the software known as Matlab programming or software (Image J or Image ProPlus). The image captured must be calibrated before processing to get an accurate measurement.

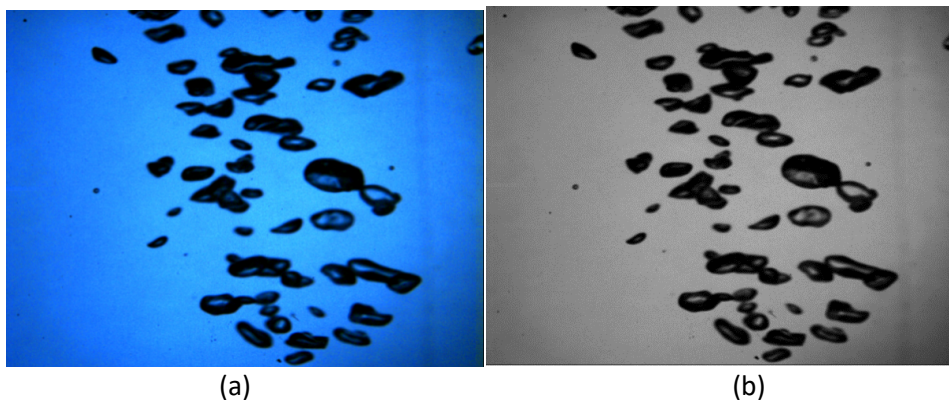


Fig. 2. (a) raw image, RGB and (b) grayscale image

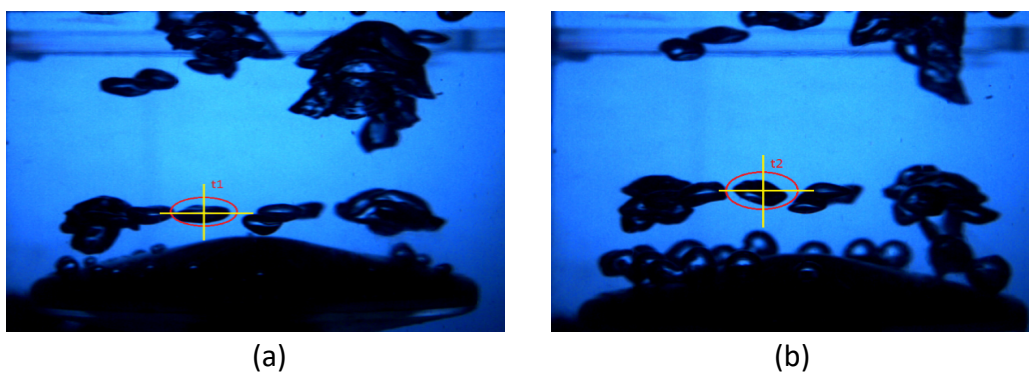


Fig. 3. Bubble velocity measurement (a) bubble at t1 (b) bubble at t2

The bubble is detected by a different range of sizes (group, according to sizes). Then, the total bubbles in the selected region is calculated to give a gas void fraction in that region. First, an image where the bubble to be tracked is calibrated according to the real size of the images captured. Then, a single bubble is tracked at times, t_1 and the bubble is measured starting from the origin place, where bubble starts to rise. Two end edge of the bubble is measured in horizontal and vertical distance. The equivalent diameter of the sphere bubble is calculated by the square root of horizontal diameter and vertical diameter, whereas the ellipsoid bubble equivalent diameter and aspect ratio, AR are obtained using equation below [10]:

$$d_{eq} = 2\sqrt[3]{a^2b} \tag{1}$$

$$AR = \frac{b}{a} \tag{2}$$

Where, a is the vertical and b is horizontal distance.

Next, as bubble move up, the images will move to the second time frame, t_2 image and the distance of bubble at t_2 is measured. The bubble velocity as it moves to point 2 is calculated by measuring the difference between two bubble distance divide by the time interval from t_1 to t_2 . Each of the bubble are tracked in the region at every image capture from high speed camera and using a high speed camera software (Phantom V.2) and also Matlab program. The bubble dispersion is calculated by measuring the distance of the bubble travel from the origin point.

Based on the area of the region, the bubbles are divided into spherical bubbles, intermediate-size bubble and large bubbles/clusters. Bubble information extraction: owing to the different sizes and characteristics of bubbles in the images, a single universal approach cannot be used to extract the size information of all the bubbles. Thus, a multilevel segmentation approach is suggested to extract the maximum possible information from the images. Image segments of bubbles are created by groups of bubbles and not by individual bubbles, such as when two or more bubbles are overlap in the image, they are detected as a large single bubble. This causes an error in measuring the size and velocity distributions of the bubbles. However, overlapping bubbles recognition techniques is applied, which only measure the in-focus bubble and remove the bubble shadow. The image processing of the bubble clusters are shown in Figure 4 and 5 below.

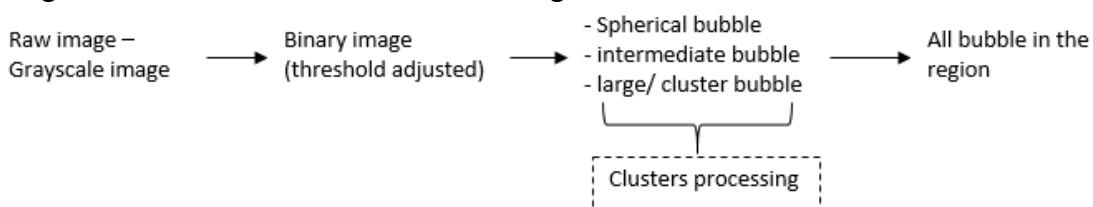


Fig. 4. Image processing techniques of large/cluster bubbles

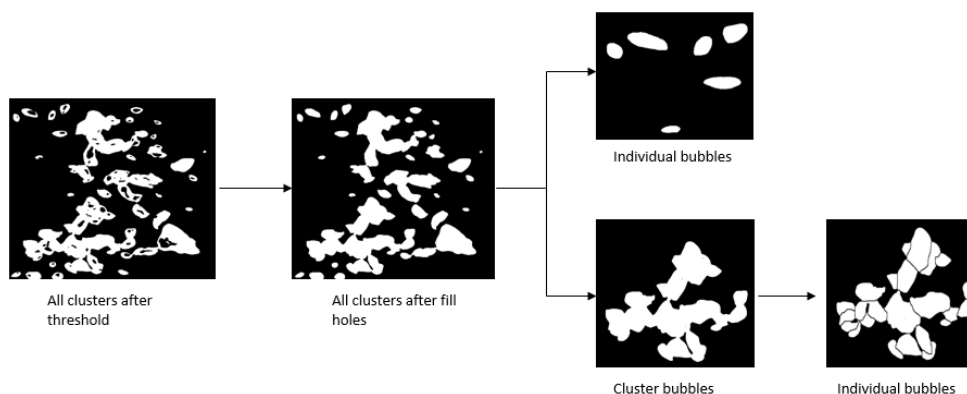


Fig. 5. Image processing of cluster bubble to form individual bubble

Even though photographic technique gives a direct measurement of the bubble, but this technique sometimes can be tedious since direct bubble measurement from the images is very time consuming, especially when a large of bubble need to be sampled. Zhu *et al.* (1999) suggested that to have a reliable statistics of bubble sizes for a systems with different sizes of bubbles, when a few thousands of bubbles need to be sampled [11].

3. Results

Figure 6 shows images of the bubbly flow when the gas is injected into the column. Initially most of the bubbles have been trapped in the region aligned vertically up near the sparger region, after sometimes bubbles are spread uniformly covering a larger portion of the whole column. The flow pattern thus being visible in the column is like a bubble plume. Visual observations indicate that the bubble size has decreased from 10 mm to 2 mm with an increase in impeller speed over the range studied here (0 rpm - 150 rpm). By increasing the rotation speed of sparger, the bubble move vigorously, thus making the regime highly dispersed and the bubbles move in zig-zag motion due to the increased water circulation in the column.

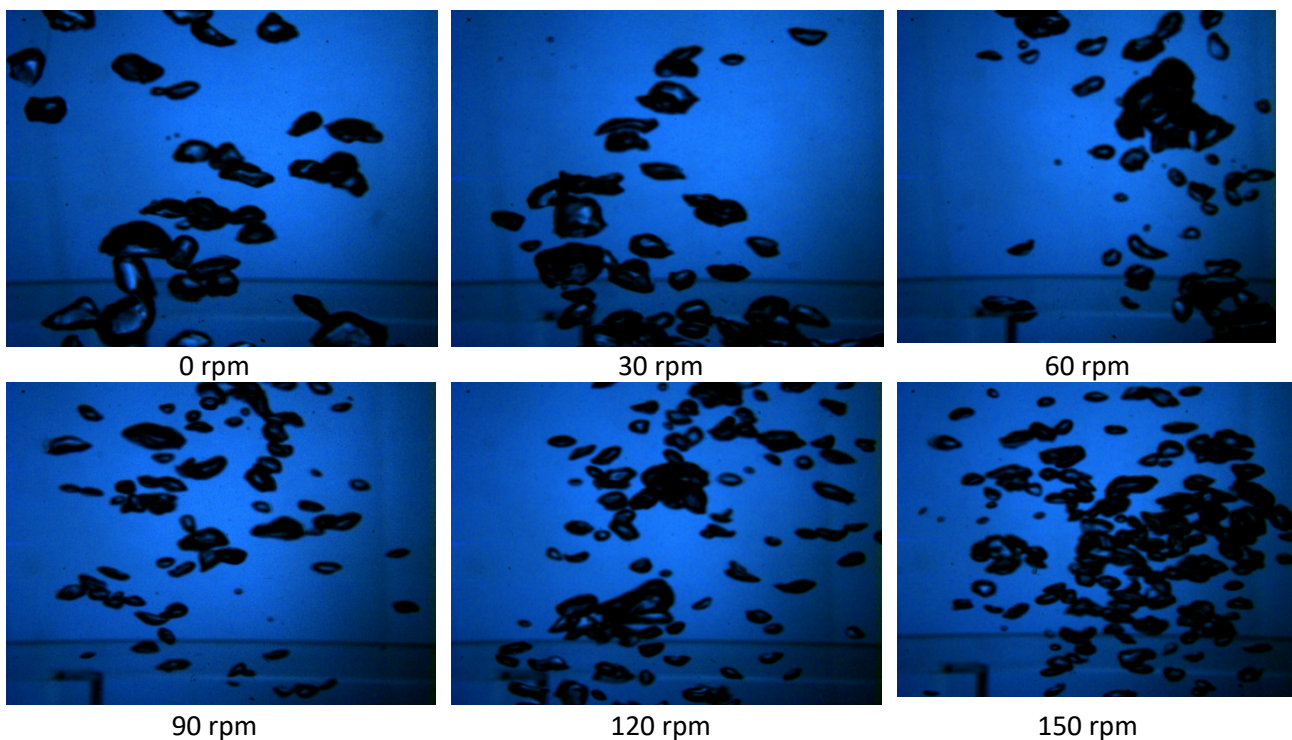


Fig. 6. Bubble images at varies rpm at constant gas rate (0.063 g/s air)

However, by increasing the gas flow rate the bubbles begin to grow in size and large bubble appear to coexist with the smaller ones as shown in Figure 7. The uprising bubbles begin to exhibit also a reciprocate movement which retards their upward movement enhancing coalescence. Increase in gas flow rate injection into bubble column, coarser bubbles are immediately released from the sparger's hole because of high buoyancy and the bubbles face more resistance to move in upward direction as well as high residence time in the column. A presence of large bubbles, formed by coalescence of the small bubbles and bearing a higher rise velocity hence leading to relatively lower gas holdup [12]. These resulting in more mixing caused by the interaction of phases and hence increase in mass transfer as well as increase the turbulence in the column. This leads to increase in bubble migration to the surrounding liquid. The bubbles size are uniform as their size are almost

similar and they move all together with little collision among bubbles and the liquid is circulated by the bubbles. Bubble size can be increased through coalescence, which two or more bubbles coming together. An increase in sparger's rotation speed yields a smaller bubble size due to a decrease in surface tension.

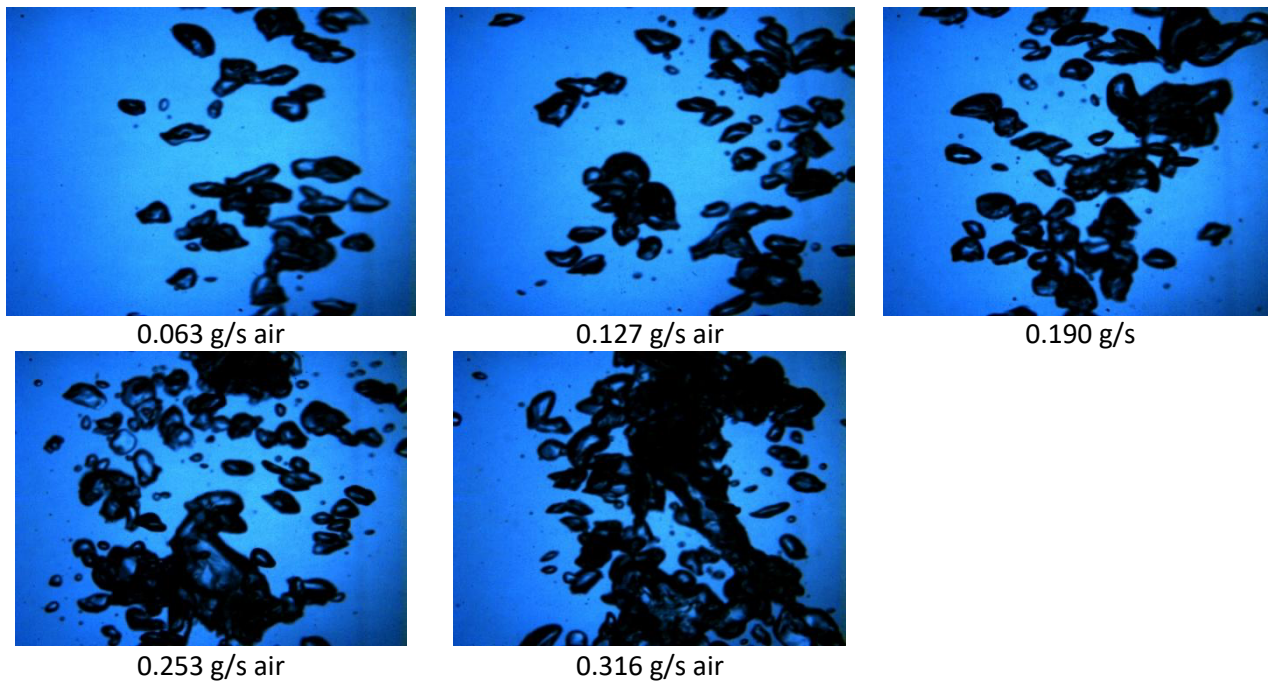


Fig. 7. Bubble images at varies gas rate

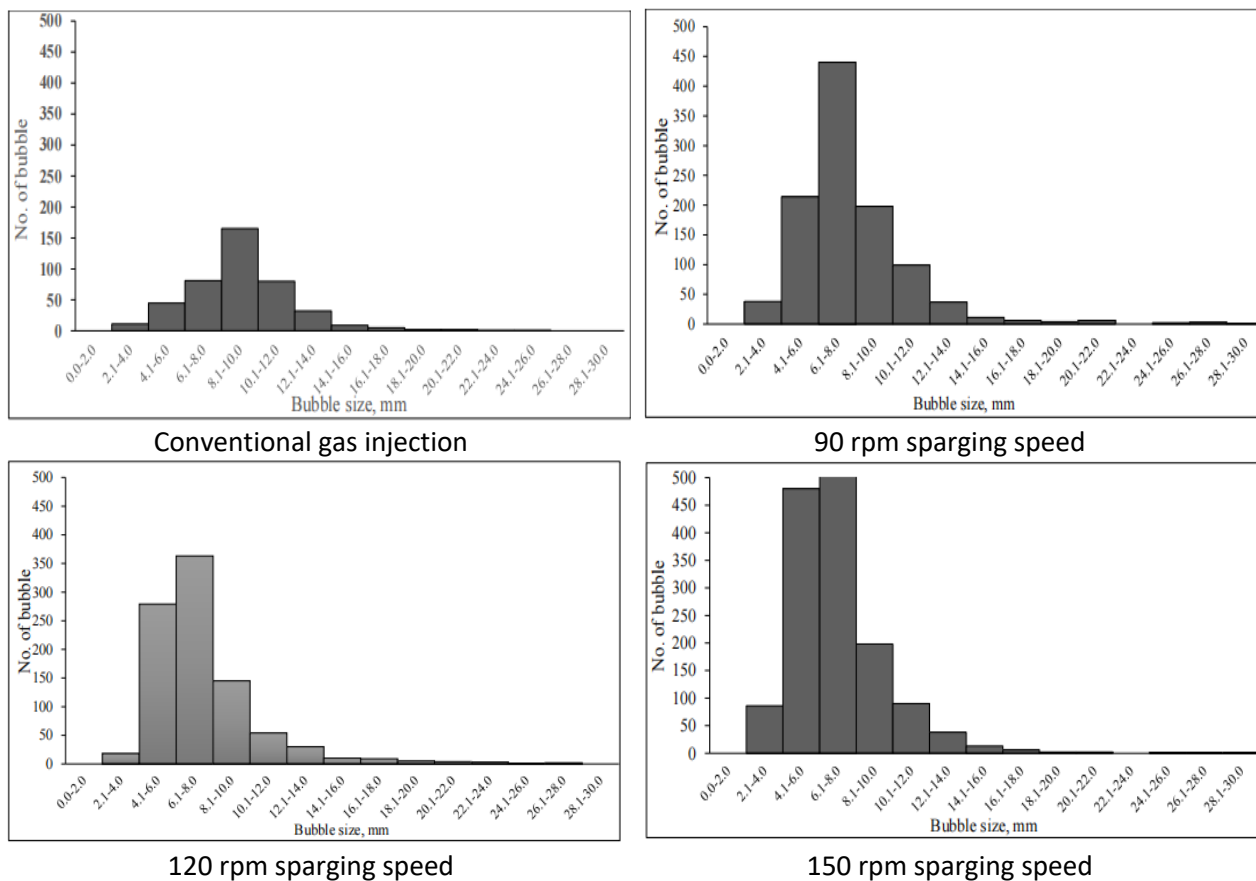


Fig. 8. Bubble population at conventional gas injection, 90 rpm, 120 rpm and 150 rpm sparging speed

From Figure 8, the results shown that the bubble population is increase as the sparger rotating speed increase from 30 rpm to 150 rpm. Besides that, the size of the bubble also reduces as the rotating speed is increase. As the rotating sparger speed increase to 150 rpm, the bubble size reduced from 12mm to 4 mm. Uniform bubble size distribution of small bubbles may increase the gas holdup and mass transfer area in bubble column [13]. The population of the bubbles is higher as the sparger’s rotation speed increase due to the formation of the bubble is uniform, with more smaller bubbles. Besides that, the size of the bubble also reduces as the rotating speed is increased. As the rotating sparger speed increases to 150 rpm, the bubble size reduced from 12 mm to 4 mm. Uniform bubble size distribution of small bubbles may lead to an increased in the void fraction that contributes to an enhanced interfacial area. Size of the bubble region at which the turbulence intensity around the bubble is enlarged depends on the bubble diameter. As the bubble diameter increases, the region of turbulence intensity also increases.

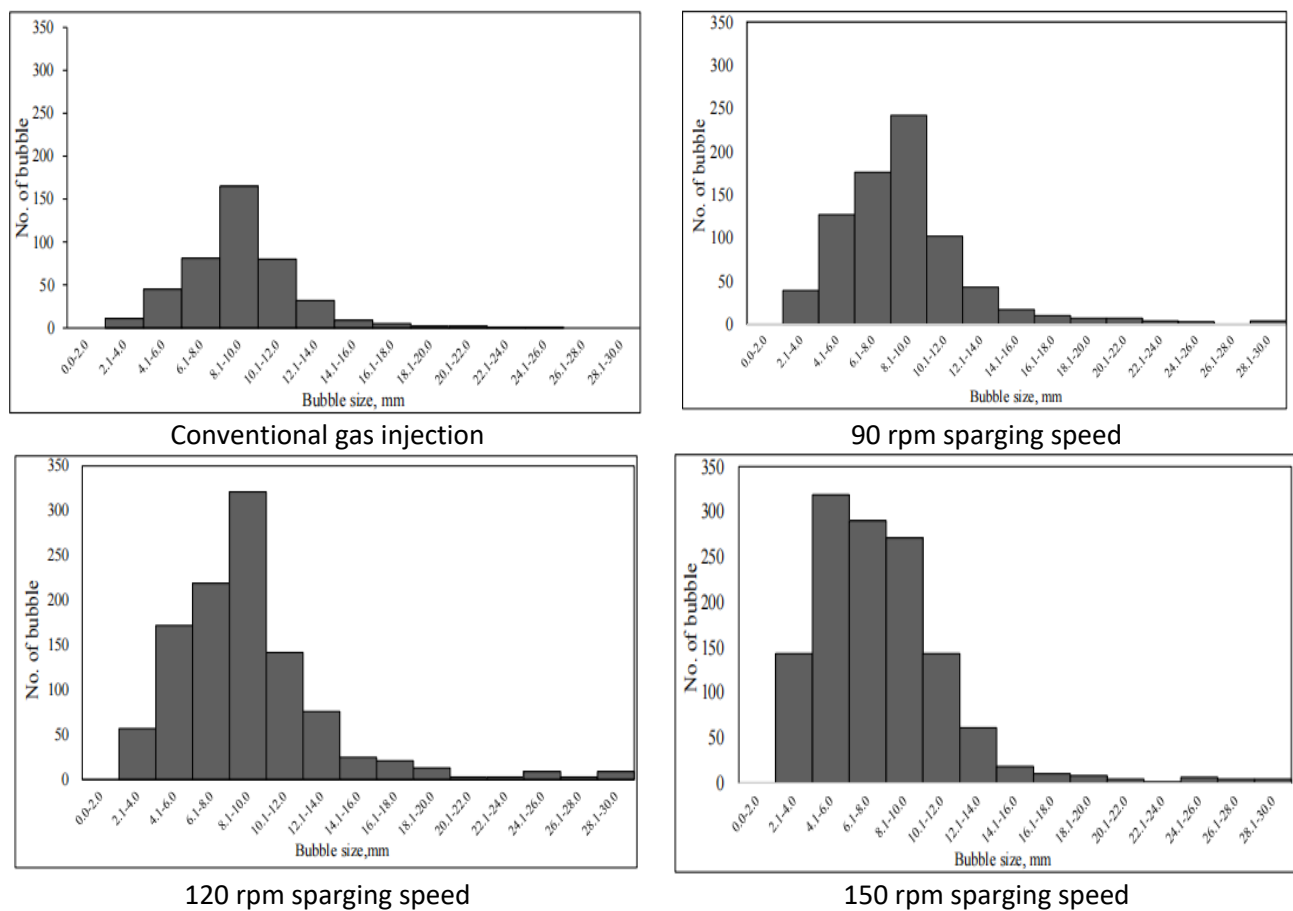


Fig. 8. Bubble frequency of air injection rate at 0.253 g/s

Figure 9 shows the bubble rising velocity affected by the bubble size, where the results from this work agreed well with the literature for air-water system; bubble rising velocity increases as the bubble size increases for conventional gas injection. This data is gathered by using ImageJ software from bubbly flow image capturing. The values of swarm bubble rising velocity have similar trends but were higher compared with the terminal velocity given by Clift *et al.* (1978)[14] and Talaia (2007)[15] for isolated bubble with diameter ranging from 1 mm to 10 mm. This can be explained by the fact that the trailing bubbles in the wake of the leading bubble rise faster than isolated bubbles due to drag reduction. Apart from that, for swirl gas injection at 90 rpm of sparger’s rotating speed,

the bubble size generated is about 3 mm to 8 mm compared to other conventional gas injection; the bubble size produced varies in size up to 20 mm, depending on the operating conditions.

Furthermore, large bubble has high rising velocity because larger bubble has the larger buoyant force compared to the smaller bubble. The bubble rise velocity depends on the diameter, as the diameter increases the air bubbles become flattened ellipsoids or any oscillate from oblate to prolate form. At a constant gas flow rate, by increasing the rotating speed from 90 – 150 rpm, the average bubble velocity reduces as the velocity is easily dissipated to the surrounding far from center region of bubble column. The average bubble rising velocity is higher in the center region of the column, and it reduces as it far from the center.

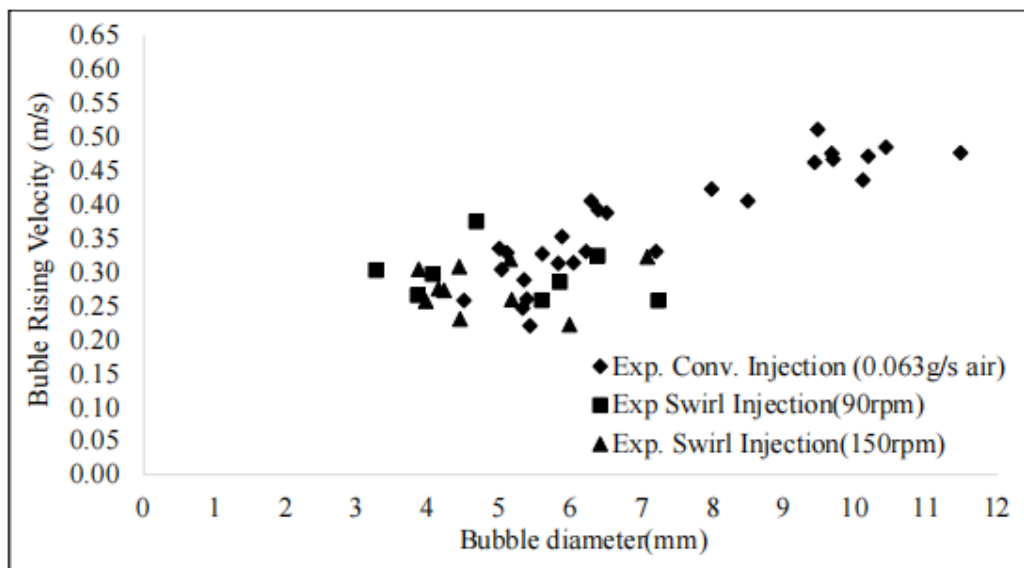


Fig. 9. Comparison of bubble velocity effect on the bubble size

However, smaller bubbles have more migration distance than larger bubbles. As the sparger rotating speed is increased, the dispersion distance of the bubble increases as the bubble moves to the top of the column. At low rotating sparger speed, the sparger dragged the bubbles away from the gas feed orifice into a spiral. Shear forces in the fluid surrounding the sparger distorted these bubbles into a crescent shape. Bubbles on the periphery of the mixing area were pulled in toward the center and were swept into the sparger region.

4. Conclusions

Swirling bubble can enhance the mixing between air and water as well as giving larger dispersion of bubble in the air water system. From this study, the efficiency of the air-water mixing is increased, thus gives knowledge that by inducing swirl bubble in the flow, we can enhance the performance of the bubbly flow process.

Acknowledgement

The authors would offer acknowledgement to the University Malaysia Sarawak (UNIMAS) Grant Dana Principal Investigator (DPI) - 02(DP123)/999/2013(06) and Centre for Automotive Research and Electric Mobility (CAREM), UTP for facilitating in these experiments.

References

- [1] Hlawitschka, Mark W., Kováts, P., Dönmez, B., Zähringer, K., Bart, H. J. (2022). Bubble motion and reaction in different viscous liquids. *Experimental and Computational Multiphase Flow*. Vol. 4, No. 1, 2022, 26–38. <https://doi.org/10.1007/s42757-020-0072-4>
- [2] Yoshimoto Kenjo & Saito Takayuki (2010). 3-dimensional liquid motion around a zigzagging ascent bubble measured using tomographic Stereo PIV. 15th Int Symp on Applications of Laser Techniques to Fluid Mechanics Lisbon, Portugal, 05-08 July, 2010. <http://ltces.dem.ist.utl.pt/LXLASER/lxllaser2010/upload/1627nisnjp2.12.1.Full1627.pdf>
- [3] Azzopardi, B., Zhao, D., Yan, Y., Morvan, H., Mudde, R. F., & Lo, S. (2011). *Hydrodynamics of Gas - Liquid Reactors: Normal Operation and Upset Conditions*, New York: John Wiley & Sons.
- [4] Agrawal, K. S. (2013). Bubble dynamics and interface phenomenon. *Journal of Engineering and Technology Research*, 5(3), 42–51.
- [5] Muilwijk, Corné & Van den Akker, Harry E.A. (2021). The effect of liquid co-flow on gas fractions, bubble velocities and chord lengths in bubbly flows. Part I: Uniform gas sparging and liquid co-flow. *International Journal of Multiphase Flow*. 137.
- [6] Buwa, V., & Ranade, V. (2002). Dynamics of gas-liquid flow in rectangular bubble columns: experiments and single/multi-group CFD simulation. *Chemical Engineering Science* 57, 4715-4736.
- [7] Mudde, R., Lee, D., Reese, J., & Fan, L. (1997). Role of coherent structures on Reynolds stresses in a 2-D bubble column. *A. I. Ch. EJournal*, 913-926.
- [8] Hibiki, T., Ishii, M., & Xiao, Z. (2001). Axial interfacial area transport of vertical bubbly flows. *International Journal of Heat and Mass Transfer*, 1869-1888.
- [9] Sun, X., Kim, S., Cheng, L., Ishii, M., & Beus, S. (2004). Interfacial structures in confined cap-turbulent and churn-turbulent flows. *International Journal of Heat and Fluid Flow*, 44-57.
- [10] Besagni G., & Inzoli F. (2016). Bubble size distributions and shapes in annular gap bubble column. *Experimental Thermal and Fluid Science*, 74, 27-48.
- [11] Zhu, Y., Bandopadhyay, P., Wu, J., & Shephard, I. (1999). On the bubble size distribution in a stirred vessel with gas sparging.
- [12] Joshi, J., Vitankar, V., Dhotre, A., & Ekambara, M. (2002). Coherent flow structures in bubble column reactors. *Chemical Engineering Science*, 3157-3183.
- [13] Loubiere, K., & Hebrard, G. (2003). Bubble formation from a flexible hole submerged in a inviscid liquid. *Chemical Engineering Science*, 58, 135-148.
- [14] Clift, R., Grace, J., & Weber, M. (1978). *Bubbles, Drops, and Particles*. London: Academic Press.
- [15] Talaia, M. R. (2007). Terminal Velocity of a Bubble Rise in a Liquid Column. *Engineering and Technology*, 22(5), 264–268